Modeling the effect of the increase in the actuation voltage on the dynamic behavior of a RF MEMS switch

Majid Jamshidzadeh; Director of master's thesis Dr.Jasmina Casals***

**Master in Nanotechnology University of Barcelona, jamshidzade@gmail.com*

***Professor Associate in university polytechnic Barcelona,jasmine.casals@upc.edu*

***Abstract*—In the past few years many reports have demonstrated the development of RF-MEMS switches considering the mechanical, electrical and chemical behaviors separately. However there are a few works which address the whole aspects of RF-MEMS in a single model. In this paper we present such a numerical model to characterize the dynamic behavior of RF-MEMS switches. The goal is to analyze the effect of an increase in the actuation voltage on the insertion losses of the RF switches. The numerical results will be compared to the experimental data obtained from previous prototypes.**

***Index Terms*—RF-MEMS, Stiction, Capillary Force, Casimire Force, Van der Waals Force, Ohmic contact, charging contact**

I. INTRODUCTION

The RF-MEMS switches are micro-electro-mechanical systems (MEMS) which have unique switching capabilities in a large frequency band. The outstanding features of these devices are high insulation and low power consumption in addition to a very simple power supply circuit.

The main applications of RF-MEMS include the wireless communication industry (e.g. wireless handsets, wireless LANs) and global positioning systems. Their actuation forces are obtained by electrostatic, magneto static, piezoelectric or thermal interactions. The switches discussed in this work are electrostatically actuated which has a very low switching time (2-30μs). The electrostatic force is induced by an applied voltage between the cantilever and a bottom electrode. This force pushes the cantilever to make contact with the electrode allowing the signal transmission.

The RF switches can be classified according to their: RF circuit configuration, mechanical structure and contact type. One of the most common circuit configurations is the single pole-single throw connected in series or in parallel. The most used mechanical structures to build RF switches are the cantilever and the bridge; and the more common type of contacts are the capacitive ones (metal-insulating material-metal) and the resistive ones (metal-metal).

Commonly the electrostatic actuation is preferred to other types due to lower power consumption and consequently less power loss in the process. An important aspect to design electrostatic RF switches is to decrease the switching time and the actuation voltage. Towards this goal, the mechanical behavior of the system should be analyzed carefully since it plays an important role. For example the design and development of a switch with low spring constant and damping force results in a less power consumption and faster switching behavior.. Some background about the topic will be presented in the second section, and then a brief description of the development of our switch is given in the third section. The mechanical, electrical and chemical components are discussed in section four. The results are presented in section five and the last section concludes the paper.

II. BACKGROUND

The electrostatic actuation model of clamped-clamped beam for double ended tuning fork oscillators has been developed recently [Ref.1] which considers two cases: (i) static case and (ii) dynamic case. A good explanation about evaluation energy in the term of the actuation AC dynamic pull-in algorithm was found. This model has been extended for two types of RF switches and it was demonstrated that the algorithm can be applied for both switches [Ref.2]. However the chemical and contact forces were not included in this model. In another study, the characterization of RF-MEMS switches based on instrumentation typically available in microwave laboratories was evaluated and also mention that the mechanical model used in this paper was a simplified linear lumped model[Ref.3]. Switching and release times of different RF-MEMS DC-contact switches fabricated by FBK-first have been also measured in this work.

Here, the main objective is to develop the electrostatic actuation model [Ref.1] for reproducing the experimental results reported by Llamas et al.[Ref.3]. For this reason, the contact and chemical aspects of RF switches are introduced in the developed model. We also aim to demonstrate that our

the process provides also a thin gold layer to coat exposed metal contact that can also be used as a floating electrode .

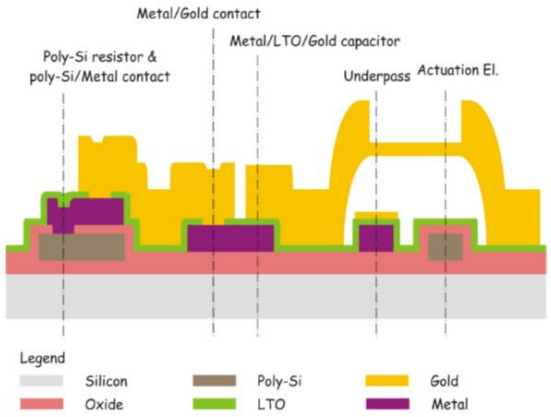

Fig 2. Schematic cross section of the micro-switch process

The cross section of the ohmic contact corresponds to Underpass, with two differences: (1) behind the purple metal layer (TiN) there is the polysilicon squares that arise the metal to make the bumps that ensure the good contact and (2) there is a VIA in the green LTO layer behind the metal (FLOMET) in order to make a ohmic contact as in section Metal/Gold contact between the Metal TIN + Flomet and the Bridge. The section Actuation El. corresponds to the electrodes. Just one difference is that on the bridge (between Actuation El. and Underpass) there is an additional thickness of gold (CPW). The dielectric is the layer OXIDE+LTO. Table 1 indicates the specification of the layers for the fabrication of switches.

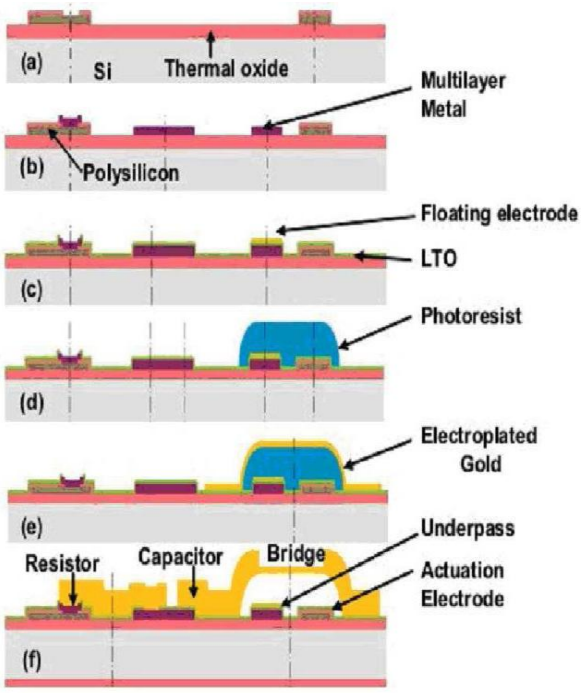

Fig 3. Schematic fabrication of the micro-switch process

.

Physical Layers	Thickness	Sheet Resistance	Dielectric constant	stress	Stress grad	Young modulus
Name	Nm	Ω/sq		Mpa	Mpa/μm	GPa
Substrate	525±15 (1)	>5000(5)	13.5			
Field oxide	1000±30		3.94	-274		
Poly-silicon	630±15	1584±52		-260		
TEOS	300±10		3.94	36		
TiN	80±5(2)					
Aluminium	440±25	0.0654 ±0.0011(6)				
TiN	110±15 (3)					
LTO	100±5		3.94	150		
FLOMET	150±5(7)	0.126± 0.010				
Spacer	3000±200					
Bridge	1800±200(4)	0.022± 0.004		120	6.95±0.4(8)	98.5±6
CPW	3000±400(4)	0.0055 ±0.0008		120		98.5±6

Table 1. Dimensions, tolerance and properties of the structural layers. (1)micron (2) 30nm of Ti as adhesion-layer (3) 30nm of Ti as adhesion-layer (4) 2.5nm of Chrome as adhesion-layer (5) Ωcm (6) applies to metal multilayer (7) 5cm Chrome as adhesion layer (8) A beam bends down (toward wafer), N.B Sign convention for stress values: (+) tensile (-) compressive.[FBK-first institute]

Microelectromechanical devices are fabricated on high resistivity (5 kΩ·cm) p-type silicon substrates, and can be optionally integrated with passive components. An initial thermal oxidation (1000 nm) is followed by the deposition of a high resistivity LPCVD polysilicon (630 nm) layer that is later patterned to create the actuation electrodes and biasing resistors. A 300 nm thick TEOS oxide is deposited and patterned to open the contact holes. Subsequently, the underpass metal lines, which connect the central conducting line of the coplanar waveguides (CPW) under the switches, are patterned on a complex sputtered metal multilayer composed of a Ti-TiN (30– 50 nm) diffusion barrier, a low resistivity Al:Si layer (440 nm) and a capping layer of Ti-TiN (30–80 nm). Thus, this multilayer equals the thickness of the previously deposited polysilicon film. Later, a layer of 100 nm of Low Temperature LPCVD Oxide (LTO) is deposited and via holes is patterned on it. The switch reliability will strongly depend on the quality

The residual-stress-caused strain energy can be expressed

$$W = w_b \int_{-h/2}^{h/2} dz \int_{-L/2}^{L/2} \tilde{W} dx = \sigma w_b \int_{-h/2}^{h/2} dz \int_{-L/2}^{L/2} \varepsilon dx$$
$$W = \sigma w_b L h \varepsilon = \frac{\sigma w_b h \pi^2}{4L} c^2 \quad (8)$$

We now add this to the total potential energy, which we have already derived for the case of no residual stress. Considering the case of a point load in the center of the beam

$$U = W - N(f) = \frac{E w_b}{2} \int_{-h/2}^{h/2} \int_{L/2}^{L/2} \varepsilon^2{}_T dz dx - N(f) \quad (9)$$

$$U = \frac{E w_b h \pi^4 (8h^2 + 3c^2) c^2}{96 L^3} + \frac{\sigma w_b h \pi^2}{4L} c^2 - N(f) \quad (10)$$

The load-deflection characteristics for the clamped beam with residual stress by minimizing this expression with respect to the variational parameter, *c* applying the principle of virtual work is:

$$F = \frac{\pi^4}{6} \frac{E w_b h^3}{L^3} c + \frac{\pi^2}{2} \frac{\sigma w_b h}{L} c + \frac{E w_b h}{L^3} c^3 \quad (11)$$

From equation 11, we can derive the equivalent stiffness which is nonlinear

$$K_{eff} = \frac{F}{x} = K_1 + K_3 x^2 = \frac{\pi^4}{6} \frac{E a_{cros} h^3}{L^3} + \frac{\pi^2}{2} \frac{\sigma a_{cros} h^3}{L} + \frac{\pi^4}{8} \frac{E a_{cros} h}{L^3} x^2$$
$$K_1 = \frac{\pi^4}{6} \frac{E a_{cros} h^3}{L^3} + \frac{\pi^2}{2} \frac{\sigma a_{cros} h^3}{L}, K_3 = \frac{\pi^4}{8} \frac{E a_{cros} h}{L^3} \quad (12)$$

Where a_{cros} is area cross-section of the beam and, *h* is thickness of the beam, *E* is the Young's Modulus,-*L* is the length, w_b is a width of beam and σ is residual stress.

The spring constant has two constant terms (k1)-and one deflection dependent term-(k3). If k3 is significant, we have an amplitude-stiffening Duffing spring.

Width(μm)	2
thickness(μm)	3
Length (μm)	580-900
Actuation mass(pg)	4-6
Mass position (μm)	8-10
Residual stress(MPa)	120
Vibration mode	1ST
Modulus E(GPa)	98.5±6
Density ρ(kg/m^3)	1984

Table 2: Specifications of the contact beam in RF switches

With equations (9) and (10), the natural frequency of the beam for a particular oscillating mode and damping coefficient of the system are stated as[Ref.2]

$$w_n = \sqrt{\frac{K_{eff}}{M_{eff}}} \quad (13)$$

$$B_{eff} = \frac{\sqrt{M_{eff} . K_{eff}}}{Q} \quad (14)$$

Where M_{eff} is a mass effective of the beam K_{eff} is linear spring constant effective (k1) and *Q* is the quality factor of the system which depends on experimental conditions and material factors. This factor is selected as *Q= 10* for high frequencies and it can be chosen up to 100 for lower frequencies. Note that the major damping contribution arises from viscous damping rather than structural damping of the system [Ref.1].

B. Electrostatic model

Using basic electrostatics equations, the potential energy stored between the capacitor plates is defined as [Ref.2]

$$U_e(x, y, z) = \frac{\varepsilon_0 V^2}{2} \int_v |E|^2 dv \quad (15)$$

Where *V* is the potential difference between the capacitor plates ε_0 is the permittivity constant of vacuum between the plates and electrostatic field *E* is defined as:

$$E = -\nabla \psi \quad (16)$$

Where ∇ is the gradient operator and ψ is the electrostatic potential. From equation (14), the force generated by the electrostatic potential field in vacuum can be calculated as

$$F = -\nabla U_e = -\frac{\varepsilon_0 V^2}{2} |\nabla \psi|^2 \quad (17)$$

Consequently, the key problem to define the electrostatic force is solving the equation (16) for the electrostatic potential (ψ).

The typical approximation is to consider that the plate width and longitude are considerably large against the gap between

III. Conclusion

We present an analytical model to study the dynamic behavior of RF-MEMS switches. This model contributes to mechanical, electrostatic and contact behaviors of the parallel plates as the main components of RF switches. The related models are discussed respectively. The results show the effect of the beam length and actuation voltage on the switching behavior. For the longer switches, we observe the slower actuation. The response of the sample switch becomes faster as the actuation voltage increases while the effects of the rebounds are more pronounced. These behaviors agree with the experimental observations [Ref3].

Appendix

After solving the dynamic equation of the system using the modal shapes, the potential energy, mass and force (associated with the spring constant) are obtained as follows using the Maple software:

$$\begin{aligned} MASS = dens\,A\,e^{-9.4L}\big(&-2.7\,e^{9.4L} + 0.3\,e^{18.9L} + 60.8\,L\,e^{9.4L} \\ &- 0.01\cos(4.7L)\,e^{14.1L} - 0.01\sin(4.7L)\,e^{14.1L} - 0.04 \\ &+ 1.36\cos(4.7L)\,e^{4.7L} - 1.5\sin(4.7L)\,e^{4.7L} \\ &+ 12.9\cos(4.7L)\sin(4.7L)\,e^{9.4L} + 1.4\cos(4.7L)^2\,e^{9.40L}\big) \end{aligned}$$

$$\begin{aligned} POTENTIAL\ ENERGY\ OF\ THE\ SYSTEM = {} & 2.1\cdot 10^{-19}\,E\,In\,q(t)^2\big(-4.8 \\ &\cdot 10^{19}\,e^{9.4L} + 3.8\cdot 10^{15}\,e^{18.9L} + 7.3\cdot 10^{22}\,L\,e^{9.4L} + 1.6 \\ &\cdot 10^{19}\cos(4.7L)\,e^{14.1L} + 1.4\cdot 10^{19}\sin(4.7L)\,e^{14.1L} - 4.8\cdot 10^{19} \\ &- 1.6\cdot 10^{21}\cos(4.7L)\,e^{4.7L} + 1.8\cdot 10^{21}\sin(4.7L)\,e^{4.7L} + 1.5 \\ &\cdot 10^{22}\cos(4.7L)\sin(4.7L)\,e^{9.4L} + 1.7\cdot 10^{21}\cos(4.7L)^2\,e^{9.4L}\big) \\ &e^{-9.4L} + \frac{1}{L}\Big(1.6\cdot 10^{-16}\,E\,A\,q(t)^4\big(-2.5\cdot 10^{7}\,e^{9.4L} \\ &+ 2025.\,e^{18.9L} + 3.8\cdot 10^{10}\,L\,e^{9.4L} - 7.6\cdot 10^{6}\cos(4.7L)\,e^{14.1L} \\ &+ 8.5\cdot 10^{6}\sin(4.7L)\,e^{14.1L} - 2.5\cdot 10^{7} + 9.5\cdot 10^{8}\cos(4.7L)\,e^{4.7L} \\ &+ 8.5\cdot 10^{8}\sin(4.7L)\,e^{4.7L} - 8.07\cdot 10^{9}\cos(4.7L)\sin(4.7L)\,e^{9.4L} \\ &- 9\cdot\cos(4.7L)^2\,e^{9.4L}\big)^2\big(e^{-9.4L}\big)^2\big) + 1.8\cdot 10^{-8}\,P\,q(t)^2\big(-2.5 \\ &\cdot 10^{7}\,e^{9.4L} + 2025.\,e^{18.9L} + 3.8\cdot 10^{10}\,L\,e^{9.4L} - 7.6 \\ &\cdot 10^{6}\cos(4.7L)\,e^{14.1L} + 8.5\cdot 10^{6}\sin(4.7L)\,e^{14.1L} - 2.5\cdot 10^{7} \\ &+ 9.5\cdot 10^{8}\cos(4.7L)\,e^{4.7L} + 8.5\cdot 10^{8}\sin(4.7L)\,e^{4.7L} - 8.07 \\ &\cdot 10^{9}\cos(4.7L)\sin(4.7L)\,e^{9.4L} - 9\cdot 10^{8}\cos(4.7L)^2\,e^{9.4L}\big)\,e^{-9.4L} \end{aligned}$$

Where L is the length of the beam.

Acknowledgment

I am heartily thankful to my supervisor, Dr.Jasmina Casals, whose encouragement, guidance and support from the initial to the final level enabled me to develop an understanding of the subject

The authors acknowledge a fruitful discussion with Dr. Amir Abdollahi. Lastly, I offer my regards and blessings to all of those who supported me in any respect during the completion of the project.

References

[1] A.Fargas"Stable Electrostatic Actuation of MEMS Double-ended Tuning Fork oscillators", master thesis 2001

[2] A.Fargas etc al."Modeling the electrostatic actuation of MEMS", IOC-DT-P-2005-18,2005

[3] M.A.LIamas etc al."Characterization of Dynamics in RF-MEMS Switches",TSC,UPC,DEEEA,FBK-irst,2009

[4] M.A.ALam etc al."Achieving Full-Scale Simulation Grained Model",PRISM,PURDUE,2010

[5] D.Peroulis etc al."Electromechanical Considerations in Developing Low-Voltage RF-MEMS Switches" IEEE VOL.51,NO1 2003

[6] F.De Flaviis,R.Coccioli"Combined Mechanical and Electrical Analysis of a RF-MEMS",Irvine,CA 936697-2625,2009

[7] ZHAO Yapu"Stiction and Anti-Stiction in MEMS And NEMS" ACTA MECHANICHA SINICA VOL19 NO1,2003

[8] R.Marcelli etc al."Mechanical Modeling of Capacitive RF-MEMS shunt Switches",CNR-IMM Roma,2009

[9] James C.M.Hwang"Reliability of Electrostatically Actuated RF-MEMS Switches",Lehigh university,Bethlehem,Pennsylvania18015 USA ,2009

[10] R.Marcelli etc al." Reliability of RF-MEMS Switches Due to charging effect and their circuital modelling",CNR-IMM Roma,Springer10.1007.2009

[11] ZHAO Yapu"Electromechnical model of RF-MEMS Switches" Springer DOI 10.1007,2003

[12] D.Berman etc al,"contact voltage softening of RF-MEMS gold-gold contact",journal of applied physics 108,044307,2010

[13] Enrico P.Tomansi, B.Marchetti"numerical analysis and experimental study by micro laser Doppler for the dynamic characterization of RF-MEMS switching"ABCM,VOL2-PP447-484, 2008

[14] T.Roessig"integrated MEMS Tuning Fork Oscillators for Sensor Applications",CA.Berekley 1998

[15] Brian D.Jensen etc al,"adhesion effect on contact opening dynamic in MEMS switches",journal physics 103535 ,2005

[16] A.Fargas,J.Casals-Terre"resonant pull-in condition in parallel-plate Electrostatic Actuator"journal microelectromechanical,vol16 no5,2007